Nuclear Engineering and Technology 49 (2017) 996–1005

Contents lists available at ScienceDirect

Nuclear Engineering and Technology

journal homepage: www.elsevier.com/locate/net

Original Article

Model-based predictions for nuclear excitation functions of neutron-induced reactions on $^{64,66-68}$Zn targets

M. Yiğit [a], [*], A. Kara [b]

[a] Faculty of Science and Arts, Department of Physics, E-90 Highway 7, Km Main Campus, Aksaray University, 68100 Aksaray, Turkey

[b] Faculty of Engineering, Department of Energy Systems Engineering, Prof. Ahmet Taner Kışlalı Cd. Campus, Giresun University, 28200 Giresun, Turkey

ARTICLE INFO

Article history:
Received 3 February 2017
Accepted 28 March 2017
Available online 27 April 2017

Keywords:
Cross-Section Systematic
Evaluated Data
TALYS 1.6 Code
Zinc

ABSTRACT

In this paper, nuclear data for cross sections of the ^{64}Zn(n,2n)^{63}Zn, ^{64}Zn(n,3n)^{62}Zn, ^{64}Zn(n,p)^{64}Cu, ^{66}Zn(n,2n)^{65}Zn, ^{66}Zn(n,p)^{66}Cu, ^{67}Zn(n,p)^{67}Cu, ^{68}Zn(n,p)^{68}Cu, and ^{68}Zn(n,α)^{65}Ni reactions were studied for neutron energies up to 40 MeV. In the nuclear model calculations, TALYS 1.6, ALICE/ASH, and EMPIRE 3.2 codes were used. Furthermore, the nuclear data for the (n,2n) and (n,p) reaction channels were also calculated using various cross-section systematics at energies around 14–15 MeV. The code calculations were analyzed and obtained using the different level densities in the exciton model and the geometry-dependent hybrid model. The results obtained from the excitation function calculations are discussed and compared with literature experimental data, ENDF/B-VII.1, and the TENDL-2015 evaluated data.

1. Introduction

Studies on nuclear reaction cross sections are important in a number of areas such as accelerator-driven systems, fission, fusion, dosimetry, radiation therapy, medical radionuclide production, astrophysics, cosmochemistry [1–4]. In particular, data on the cross sections of fast neutron-induced nuclear reactions are essential for understanding nuclear phenomena in structural materials irradiated by neutrons. Such data are needed to estimate the nuclear heating, nuclear transmutation rates, induced radioactivity, and radiation damage due to gas formation on potential first wall materials [5,6]. The zinc alloy is important for the nuclear science and reactor technology. In addition, cross-sectional data of incident particle energies at 14–15 MeV are of considerable importance for the design, construction, and evaluation of nuclear fusion reactors. In this energy range, there are some analytical and empirical formulae used to calculate the reaction cross section produced by neutrons, protons, and deuterons. Therefore, calculations and experimentation for nuclear reaction cross sections at levels of energy around 14 MeV have been carried out by various authors [7–11]. On the one hand, to achieve accurate data, there is a need for more cross-sectional data for incident energies around 14 MeV. The selection of suitable models for calculations of the excitation functions is very important for obtaining correct results. Nuclear-level density models have been used in statistical calculations of nuclear reactions [1,12–15]. These models play very important roles in determining nuclear reaction excitation functions. The level density is described as the total number of levels per megaelectron-volts of excitation energy. In general, nuclear codes offer a number of model options for nuclear-level density. In that context, nuclear codes can be used for obtaining nuclear cross sections for various reaction channels. The ALICE/ASH computer code [16] can be used to analyze interactions between nucleons and target isotopes. The code can calculate the excitation functions depending on the angle and energy. In addition, the code can examine some scattering parameters and residual nuclear yields with energies up to 300 MeV [16]. On the other hand, the TALYS 1.6 code [17], which provides an accurate and complete simulation of nuclear reactions in the 1-keV to 200-MeV energy range, can be used for the analysis of basic scientific measurements or to obtain data for nuclear applications [17]. Moreover, the EMPIRE 3.2 code [18], using the equilibrium and pre-equilibrium approaches, can successfully perform the determination of nuclear cross-section data. The code also performs theoretical calculations in support of nuclear data evaluation [18]. In this study, excitation functions for neutron-induced interactions of zinc material have been investigated using ALICE/ASH [16], TALYS 1.6 [17], and EMPIRE 3.2 [18] nuclear code programs and cross-section systematics [7–11,19–26].

---

[*] Corresponding author.
E-mail address: mustafayigit@aksaray.edu.tr (M. Yiğit).

http://dx.doi.org/10.1016/j.net.2017.03.006

2. Calculations and methods

2.1. Nuclear cross-section calculations

Many theoretical models have been developed to understand the nuclear reaction mechanisms such as compound, pre-compound, and direct mechanisms. The low energy portion of the nuclear excitation curve is dominated by the equilibrium nucleus process. By contrast, the high-energy tail portion of the nuclear excitation curve of reactions produced by light target nuclei and medium energy incident particles has been one of the important signatures of pre-equilibrium process [27]. The cross-section calculations in this study have been carried out using the exciton model [28,29] and the geometry-dependent hybrid (GDH) model [30], including the pre-equilibrium reaction mechanisms. In addition, for neutron-induced (n,2n) and (n,p) reactions, empirical and semiempirical models proposed by various authors are used to obtain cross-section values at 14–15 MeV energy. In the GDH calculations, the initial exciton number is taken as $n_0 = 3$. The Fermi gas model (FGM) with the $\alpha = A/11$ level density parameter, and the superfluid nuclear model (SFM) [31] are used to calculate the cross sections in the GDH model. Furthermore, excitation function calculations were carried out using the enhanced generalized superfluid model (EGSM) [32], the constant temperature model (CTM) + FGM [33], the backshifted FGM (BSFGM) [34], and the generalized superfluid model (GSFM) [35,36] in the exciton model. Therefore, a comparison of the different models for the nuclear-level density and the cross-section systematic calculations is presented in this paper to describe the best approach.

2.2. EMPIRE 3.2 code

This code [18] is a modular system of reaction codes that is extensively used for model and data evaluation investigations of nuclear reactions. The incident particle in this code can be a nucleon, triton, deuteron, photon, ^{3}He, ^{4}He, or ions. The pre-equilibrium nuclear reaction mechanism in the code is defined by the exciton model [28], based on the solution of the equation [37] proposed by Cline [38] and Ribansky and Oblozhinsky [39].

$$\begin{aligned}-q_{t=0}(n) &= \lambda_+(E,n+2)\tau(n+2) + \lambda_-(E,n-2)\tau(n-2)\\ &\quad -[\lambda_+(E,n) + \lambda_-(E,n) + L(E,n)]\tau(n)\end{aligned} \tag{1}$$

where the term "$q_t(n)$" presents the initial occupation probability for compound nuclei in the nuclear state with the "n" exciton number. The denotation "L(n, E)" symbolizes the total emission rate integrated over the emission energy for γ-rays and particles. "$\lambda_-(E, n)$" and "$\lambda_+(E, n)$" represent transition rates of decay to neighboring nuclear states [18].

The pre-equilibrium spectra in the code can be written as follows:

$$\frac{d\sigma_{a,b}}{d\varepsilon_b}(\varepsilon_b) = \sigma^r_{a,b}(E_{inc})D_{a,b}(E_{inc}) \times \sum_n W_b(E,n,\varepsilon_b)\tau(n) \tag{2}$$

where $\sigma^r_{a,b}(E_{inc})$ represents the nuclear cross section of the (a, b) reaction, the term $W_b(E, n, \varepsilon_b)$ corresponds to the emission probability of a particle of "b" type (or γ ray) with "ε_b" energy from a nuclear state with "n" exciton and "E" excitation energy of the compound nucleus, and the term $D_{a,b}$ (E_{inc}) represents the depletion factor [18].

2.3. ALICE/ASH code

This code is a modified and advanced version of the ALICE code [16]. The description of the pre-equilibrium particle emission has been made in the hybrid model and the GDH model [30]. SFM and FGM in the code can be selected for the nuclear-level density calculations. The level density for the GSFM has been calculated as follows [31]:

$$\rho(U) = \rho_{qp}(U^1)\ K_{vib}(U^1)K_{rot}(U^1) \tag{3}$$

where the term $\rho_{qp}(U^1)$ denotes the density for quasiparticle nuclear excitation and the terms $K_{rot}(U^1)$ and $K_{vib}(U^1)$ represent rotational and vibrational enhancement factors at the U^1 effective energy of excitation [16].

The level-density parameter is written as follows:

$$\alpha(U) = \begin{cases} \breve{\alpha}(1 + \dfrac{\delta W \varphi(U^1 - E_{cond})}{U^1 - E_{cond}}, & U^1 > U_{cr} \\ \alpha(U_{cr}), & U^1 \le U_{cr} \end{cases} \tag{4}$$

where the asymptotic value of the level density parameter is equal to $\breve{\alpha} = A\left(0.073 + 0.115A^{-1/3}\right)$. The term "δW" denotes the shell correction to the nuclear mass formula. $\varphi(U) = 1 - e^{(-\gamma U)}$ and $\gamma = \frac{0.4}{A^{1/3}}$ MeV^{-1}. The U^1 effective energy of excitation, the E_{cond} condensation energy, and the U_{cr} critical energy of the phase transition are equal to $U^1 = U - n\Delta_0$; $E_{cond} = 0.152\alpha(U_{cr})\Delta_0^2 - n\Delta_0$; $U_{cr} = 0.472\alpha(U_{cr})\Delta_0^2 - n\Delta_0$. The correlation function Δ_0 is equal to $12A^{-1/2}$.

Here for exciton number "n": $n = 0$ for even–even nuclei; $n = 1$ for nuclei with odd A value; $n = 2$ for odd–odd nuclei [16].

2.4. TALYS 1.6 code

The analysis and prediction of nuclear reactions can largely be performed by the TALYS 1.6 nuclear code system [17]. The code predicts the partial and total cross sections, the angular distributions, the energy spectra, the differential spectra, and recoils. The code to obtain the nuclear cross sections uses various microscopic and phenomenological nuclear-level density models. The nuclear models and level densities are described and explained in detail in the TALYS 1.6 code manual [17]. The total level density for the BSFGM [34] has been calculated with the Fermi gas expression as follows:

$$\rho_F^{tot}(E_x) = \frac{1}{\sqrt{2\pi}\sigma}\frac{\sqrt{\pi}}{12}\frac{e^{2\sqrt{\alpha U}}}{\alpha^{\frac{1}{4}}\ U^{\frac{5}{4}}} \tag{5}$$

and the total nuclear level density $\rho^{tot}(E_x)$ represents the total number of levels per megaelectron-volts around E_x.

The level density in the model is written as follows:

$$p_F(E_x, J, \Pi) = \frac{1}{2}\frac{2J+1}{2\sqrt{2\pi}\sigma^3}\exp\left[-\frac{\left(J+\frac{1}{2}\right)^2}{2\sigma^2}\right]\frac{\sqrt{\pi}}{12}\frac{e^{2\sqrt{\alpha U}}}{\alpha^{\frac{1}{4}}\ U^{\frac{5}{4}}} \tag{6}$$

and the nuclear-level density $p(E_x, J, \Pi)$ represents the number of levels per megaelectron-volts around an excitation energy E_x for a certain parity π and spin J.

The effective excitation energy is equal to $U = E_x - \Delta^{BFM}$. The energy shift is represented by

$$\Delta^{BFM} = \mathscr{X}\frac{12}{\sqrt{A}} + \delta$$

where $\mathscr{X} = 1$ for even–even nuclei; $\mathscr{X} = 0$ for nuclei with odd A value; $\mathscr{X} = -1$ odd–odd nuclei [17].

2.5. *Cross-section systematics*

The nuclear cross-section values can be calculated using formulae constructed for the different systematics. Many authors attempting to determine the accurate cross section have studied this issue and suggested empirical and semiempirical formulae using different nuclear parameters [5–11,19–26,40–44]. The nuclear cross-section systematic of the reactions induced by fast neutron can be approximately written as follows:

$$\sigma_{n,x} = C\sigma_{ne}e^{(as)} \tag{7}$$

where the asymmetry parameter value "$s = (N–Z)/A$" is generally used in the formula, and the term x is the produced particle for a nuclear reaction; "a" and "C" for the (n,x) nuclear reaction are the fitting parameters obtained by least-squares method [19].

3. Results and discussion

This study was conducted at up to 40 MeV for cross-section calculations of neutron-induced nuclear reactions such as ^{64}Zn(n,2n)^{63}Zn, ^{64}Zn(n,3n)^{62}Zn, ^{64}Zn(n,p)^{64}Cu, ^{66}Zn(n,2n)^{65}Zn, ^{66}Zn(n,p)^{66}Cu, ^{67}Zn(n,p)^{67}Cu, ^{68}Zn(n,p)^{68}Cu, and ^{68}Zn(n,α)^{65}Ni. Each reaction has a peculiar structure. Therefore, all reaction mechanisms must be interpreted separately. Comments can be seen for all reactions under different titles, as follows.

3.1. *^{64}Zn(n,2n)^{63}Zn nuclear reaction*

Fig. 1 and Table 1 present cross sections of the ^{64}Zn(n,2n)^{63}Zn nuclear reaction at energies up to 40 MeV. The excitation functions given by the different nuclear-level density prescriptions via ALICE and TALYS codes have different cross-section results. Moreover, a very good agreement exists between the ENDF/B-VII.1 [45] and TENDL-2015 [46] libraries. As can be seen in Fig. 1 and in Table 1, the results obtained using the cross-section formulae of Lu and Fink [21], Habbani and Osman [26], and Bychkov et al. [25] are higher than the measured data and other calculations at energies around 14 MeV. By contrast, the cross-section values of Luo et al. [8], Tel et al. [9], Adam and Jeki [10], and Konno et al. [11] are similar to the experimental data for the investigated reaction. The exciton model calculations performed via EMPIRE code had lower cross sections than those of the other calculations in the overall energy range. Besides this, the cross-section calculation results of the EGSM show a good harmony with the experimental data of Uwamino et al. [47] within the error bars. The experimental data of Bhatia and Tornow [50] at incident energy of 12.42–14.41 MeV show excellent harmony with the SFM predictions made using the pre-equilibrium GDH model. The excitation functions obtained using the TALYS code at 14.1–16.05 MeV showed good predictions of the measured cross sections reported by Bormann and Lammers [52] within the experimental uncertainty. The excitation functions for this reaction reach their maximum values at neutron energies of 16–24 MeV. In the maximum region, the experimental data of Cohen and White [48] and Paulsen and Liskien [49] are quite a bit higher than the other cross-section results.

3.2. *^{64}Zn(n,3n)^{62}Zn nuclear reaction*

The model calculations for the cross sections of the nuclear reaction ^{64}Zn(n,3n)^{62}Zn along with the experimental data of Vrzalova et al. [54], Soewarsono et al. [55], and Uwamino et al. [47] are shown in Fig. 2. It can be clearly seen that the model results obtained using the EMPIRE code are lower than the other data for the investigated energy range. The experimental value of 29 ± 4 mb reported by Vrzalova et al. [54] at 30.4-MeV energy is in very good agreement with the cross-section results, except for those obtained using the TENDL-2015 and EMPIRE codes. From Fig. 2 it can be seen that FGM calculations with the α = A/11 level density parameter using the pre-equilibrium GDH model in the ALICE computer code are in very good agreement with the measured cross-section data of Soewarsono et al. [55]. Excitation functions determined by

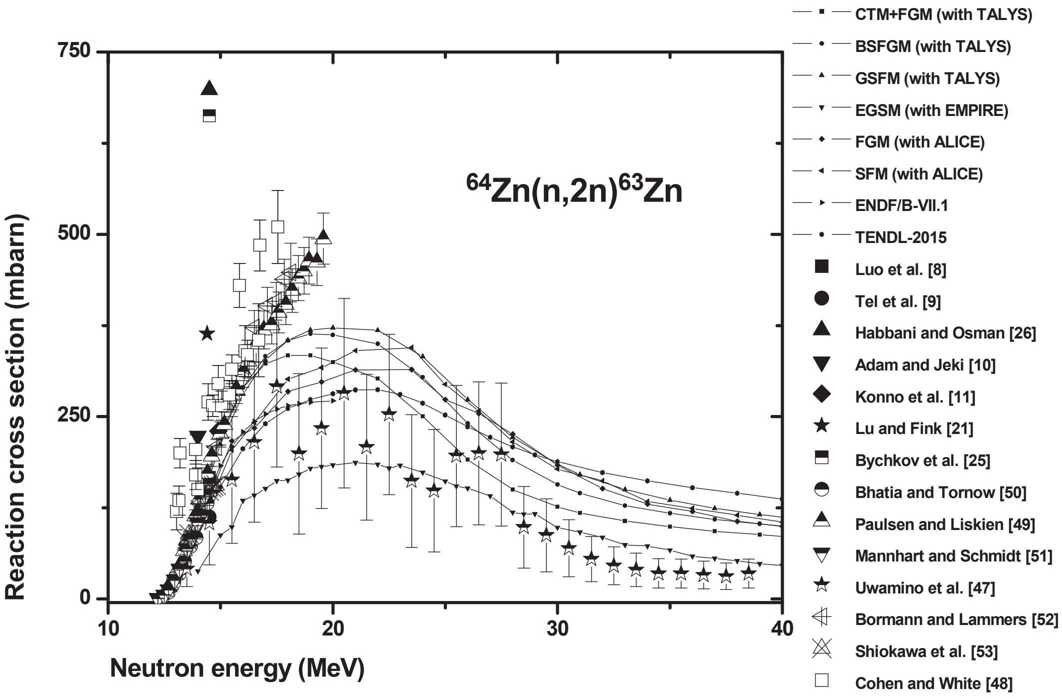

Fig. 1. Cross-section predictions and experimental data [78] for ^{64}Zn(n,2n)^{63}Zn nuclear reaction.

Table 1
The cross sections for the considered (n,2n) reactions at 14–15-MeV energy.

	Projectile energy (MeV)	Cross sections (mb) for (n,2n) reactions	
		^{64}Zn(n,2n)^{63}Zn	^{66}Zn(n,2n)^{65}Zn
Measured data	14–15	114.5; 131.1 [50] 137; 172; 196; 227 [49] 143.1 [51] 103.8 [47] 131.1; 208.1 [52] 122; 148; 153; 155; 156 [53] 150; 270; 265; 295 [48]	630; 685 [60] 758; 864 [52] 588; 618; 746; 739; 766 [61] 550 [63] 663; 738 [62]
CTM + FGM (with TALYS)	14	130.79	720.91
BSFGM (with TALYS)	14	124.51	618.63
GSFM (with TALYS)	14	119.99	535.7
EGSM (with EMPIRE)	14	38.09	407.98
FGM (with ALICE)	14.1	102.61	672.67
SFM (with ALICE)	14.1	136.24	736.86
ENDF/B-VII.1	14.5	148.12	715.52
TENDL-2015	14.5	120.54	645.7
Luo et al. [8]	14.5	166.81	544.6
Tel et al. [9]	14–15	112.42	474.03
Habbani and Osman [26]	14.5	698.22	788.4
Adam and Jeki [10]	14	223.62	595.81
Konno et al. [11]	14.9	230.42	677
Lu and Fink [21]	14.4	363.96	632.95
Bychkov et al. [25]	14.5	662.86	827.27

BSFGM, backshifted Fermi gas model; CTM, constant temperature model; EGSM, enhanced generalized superfluid model; FGM, Fermi gas model; GSFM, generalized superfluid model; SFM, superfluid nuclear model.

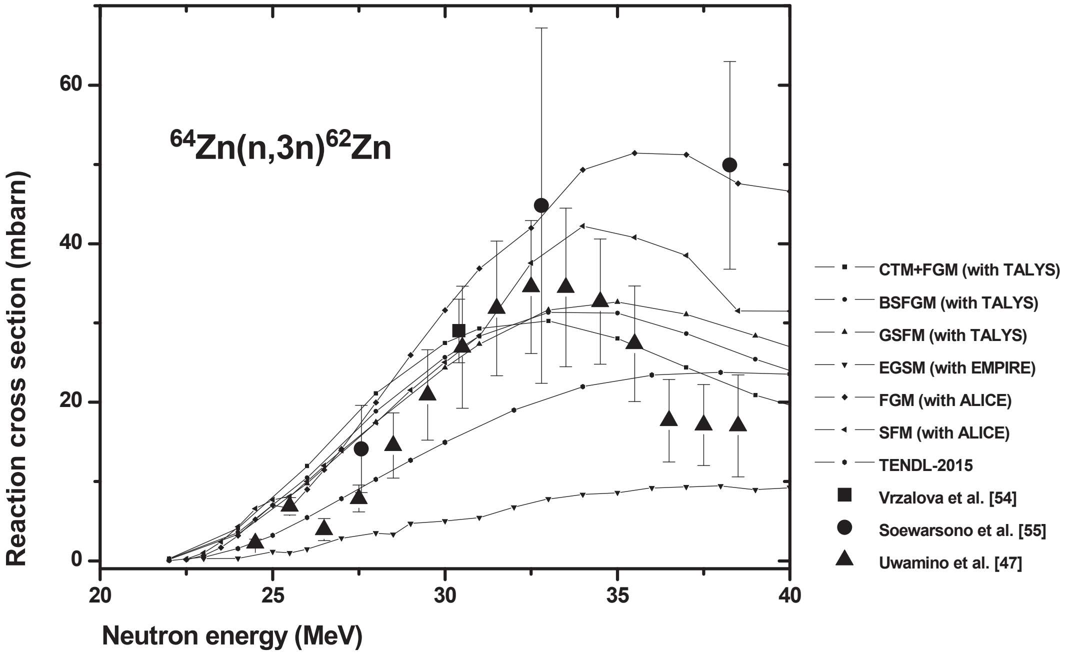

Fig. 2. Cross-section predictions and experimental data [78] for ^{64}Zn(n,3n)^{62}Zn nuclear reaction.

different level density models using the pre-equilibrium exciton nuclear model via TALYS code at 28.5–35.5 MeV energy yield an acceptable harmony with the experimental cross-section data reported by Uwamino et al. [47] within the experimental uncertainty. The calculations obtained by changing the nuclear-level density models have different cross-section data.

3.3. ^{64}Zn(n,p)^{64}Cu nuclear reaction

All cross-section data for the ^{64}Zn(n,p)^{64}Cu nuclear reaction are summarized in Table 2 and plotted in Fig. 3. The excitation functions give maximum cross sections in a neutron energy range of 5–15 MeV. In this energy region, the cross-section data, which are based on the pre-equilibrium approach of the EMPIRE code, are quite higher than those of the other excitation functions. It can be seen in Fig. 3 that the evaluated data from the ENDF/B-VII.1 and TENDL-2015 make an excellent curve with the data reported by Huang et al. [56]. By contrast, the evaluated data yield a close curve with the excitation function of Santry and Butler [57] at energies of 4.96–13.58 MeV. In addition, the cross-section data of Mannhart and Schmidt [51] are similar to the evaluated data and the exciton model predictions made with the CTM + FGM level density model.

Table 2
The cross sections for the considered (n,p) reactions at 14–15-MeV energy.

	Projectile energy (MeV)	Cross sections (mb) for (n,p) reactions			
		^{64}Zn(n,p)^{64}Cu	^{66}Zn(n,p)^{66}Cu	^{67}Zn(n,p)^{67}Cu	^{68}Zn(n,p)^{68}Cu
Measured data	14–15	164.1 [51] 134 [56] 191.7; 145.4 [52] 220; 185; 180 [58] 153; 134; 154; 139; 125 [59]	63; 74; 75 [59] 57.7; 53.8; 56.2; 59.2 [65] 69.8; 63.3 [67] 77.4 [68] 76 [66]	90; 107; 100; 117; 114 [59] 44.9; 47.3 [67] 82 [69] 43 [70]	29.3; 27.2 [67] 46 [72] 13.1; 21.9; 22.5; 16.8 [59] 11 [74] 14 [75] 4.47; 4.75; 4.66; 4.71; 4.52 [73]
CTM + FGM (with TALYS)	14	166.62	58.76	63.63	37.57
BSFGM (with TALYS)	14	130.57	59.01	81.71	40.35
GSFM (with TALYS)	14	112.65	68.69	48.85	29.36
EGSM (with EMPIRE)	14	373.84	134.31	104.7	56.17
FGM (with ALICE)	14.1	257.12	135.64	131.38	65.39
SFM (with ALICE)	14.1	225.23	102.16	98.77	51.35
ENDF/B-VII.1	14	175.16	58.41	43.63	22.72
TENDL-2015	14.5	158.72	64.36	35.26	27.37
Luo et al. [8]	14.5	182.83	69.84	44.12	28.25
Kumabe and Fukuda [24]	14	206.45	64.35	36.9	21.52
Habbani and Osman [26]	14.5	102.33	39.74	24.49	16.33
Konno et al. [11]	14.9	127.67	56.82	38.61	26.54
Ait-Tahar [7]	14	152.9	55.68	34.37	21.52
Levkovskii [19]	14	143.66	57.19	36.84	24.04
Doczi et al. [23]	14.7	128.06	61.19	42.44	29.53
Kasugai et al. [22]	14	174.26	59.18	34.39	20.06
Tel et al. [20]	14–15	69.12	33.02	23.21	16.48

BSFGM, backshifted Fermi gas model; CTM, constant temperature model; EGSM, enhanced generalized superfluid model; FGM, Fermi gas model; GSFM, generalized superfluid model; SFM, superfluid nuclear model.

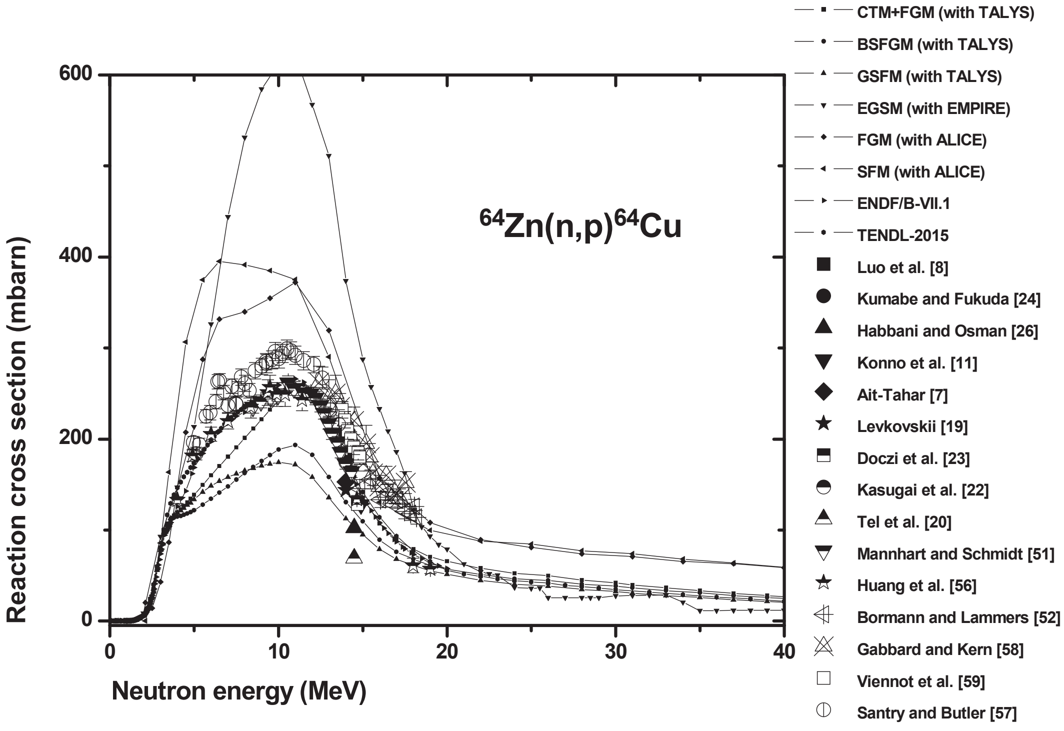

Fig. 3. Cross-section predictions and experimental data [78] for ^{64}Zn(n,p)^{64}Cu nuclear reaction.

In general, the pre-equilibrium GDH model calculations in the ALICE code are in agreement with the experimental data of Gabbard and Kern [58] and Bormann and Lammers [52]. Besides, the SFM calculations of the pre-equilibrium GDH model show a good harmony with the experimental data of Viennot et al. [59]. From Fig. 3 it can be seen that the pre-equilibrium exciton model calculations with different level density models performed using the TALYS and EMPIRE codes are consistent with each other in the energy region of 20–40 MeV. From Table 2, it can be seen that the cross-section data determined using the empirical and semiempirical formulae of Luo et al. [8], Kumabe and Fukuda [24], Konno et al. [11], Ait-Tahar [7], Levkovskii [19], Doczi et al. [23], and Kasugai et al. [22] are in agreement with the experimental data of Mannhart and Schmidt [51], Huang et al. [56], Bormann and Lammers [52], Gabbard and Kern [58], and Viennot et al. [59] at neutron energies of approximately 14 MeV.

3.4. *^{66}Zn(n,2n)^{65}Zn nuclear reaction*

Excitation curves for the ^{66}Zn(n,2n)^{65}Zn nuclear reaction are summarized in Table 1 and plotted in Fig. 4. The measured cross-section data reported by Paulsen et al. [60] exhibit a trend similar to the shapes of the excitation functions of the ENDF/B-VII.1 evaluations, and similar to the pre-equilibrium exciton model calculations performed using the BSFGM level density via TALYS code. The SFM and CTM + FGM predictions of the pre-equilibrium models are similar to the experimental data of Bormann and Lammers [52] in the energy range of 14.1–16.05 MeV. The other experimental data of Bormann and Lammers [52] yield higher results than those of the other excitation functions. The experimental data of LuHanlin et al. [61] at 14.58 MeV, 14.78 MeV, and 14.8 MeV, and the existing measured data of Wagner et al. [62] show good agreement with the ENDF/B-VII.1 data and BSFGM calculations. By contrast, the other data points of LuHanlin et al. [61] are similar to the TENDL evaluated data. The cross-section value of Csikai and Peto [63] at 14.21 MeV is in agreement with the GSFM predictions of the pre-equilibrium exciton model. The two measured data points of Vrzalova et al. [54] at energies of 30.4 MeV and 30.9 MeV show good harmony with the TENDL evaluated data. It can be stated that the pre-equilibrium approaches are dominant in the investigated excitation energy region. Excitation curves have maximum cross-section values at 15–22 MeV of neutron energy. In Table 1, the data obtained using the cross-section systematics of Luo et al. [8], Bychkov et al. [25], Lu and Fink [21], Konno et al. [11], Adam and Jeki [10], and Habbani and Osman [26] at around 14 MeV show good harmony with the evaluated data, the measured data, and the pre-equilibrium model calculations performed using the ALICE and TALYS codes.

3.5. *^{66}Zn(n,p)^{66}Cu nuclear reaction*

Fig. 5 and Table 2 show the excitation functions for the ^{66}Zn(n,p)^{66}Cu nuclear reaction. In general, the model-based calculated cross sections have maxima at incident neutron energy of 10–20 MeV. The FGM and SFM calculation results obtained by ALICE code are not consistent with the other nuclear excitation functions. From Fig. 5, it can be seen that the TENDL-2015 data and the exciton model results with BSFGM level densities determined by TALYS code yield an excellent fit with the experimental data of Smith and Meadows [64]. The ENDF/B-VII.1 evaluations and the BSFGM and CTM + FGM predictions obtained using the TALYS code have a good curve with the experimental data of Kasugai et al. [65] within the error bars. By contrast, the TENDL-2015 evaluations and the GSFM cross-section predictions are similar to the experimental results reported by Viennot et al. [59], Ghorai et al. [66], and Kielan and Marcinkowski [67]. In addition, the experimental points of Bormann et al. [68] at energies of 17–19.4 MeV are in good agreement with the exciton model results obtained using the EGSM level density in the EMPIRE code. It can be seen in Table 2 that the data determined from the cross-section formulae of Tel et al. [20] and Habbani and Osman [26] around the incident neutron energy of 14 MeV are somewhat lower than those obtained using other excitation functions. By contrast, it can be clearly seen that the cross-section predictions of Luo et al. [8], Kumabe and Fukuda [24], Konno et al. [11], Ait-Tahar [7], Levkovskii [19], Doczi et al. [23], and Kasugai et al. [22] are quite consistent with the evaluated data, TALYS predictions, and the experimental data.

3.6. *^{67}Zn(n,p)^{67}Cu nuclear reaction*

The theoretical predictions and the measured data for the ^{67}Zn(n,p)^{67}Cu nuclear reaction are shown in Table 2 and Fig. 6. It can be seen that the excitation functions of the pre-equilibrium model are highly affected when using different level densities for the calculations. The GDH model calculations with SFM and FGM level densities, and the exciton model predictions with EGSM level density show close agreement with the experimental data of

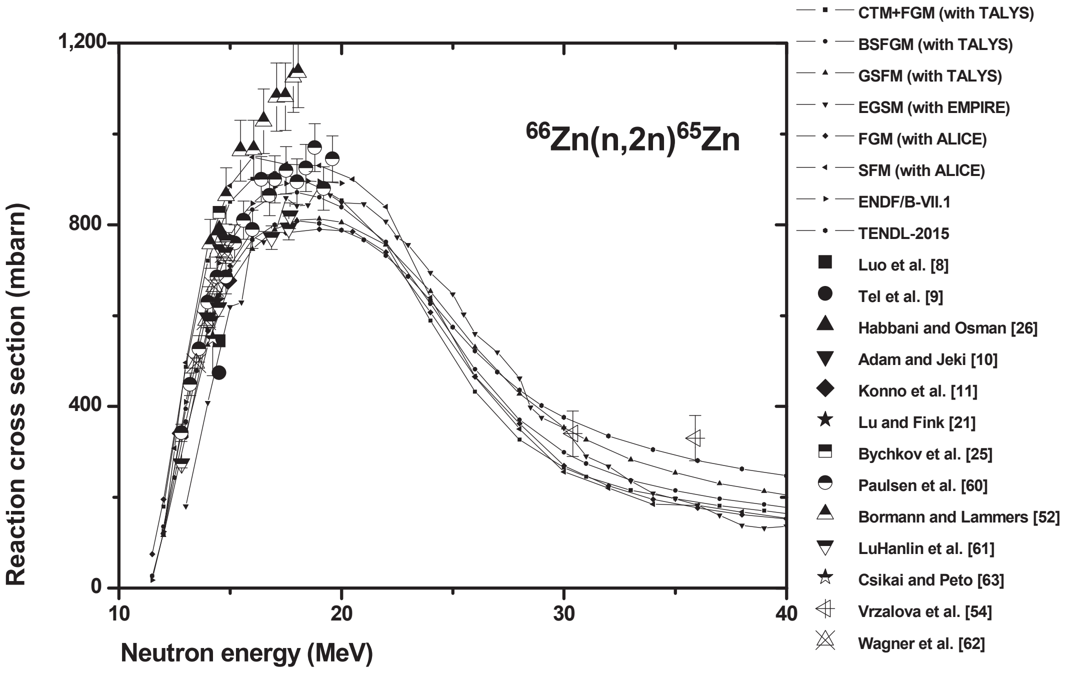

Fig. 4. Cross-section predictions and experimental data [78] for ^{66}Zn(n,2n)^{65}Zn nuclear reaction.

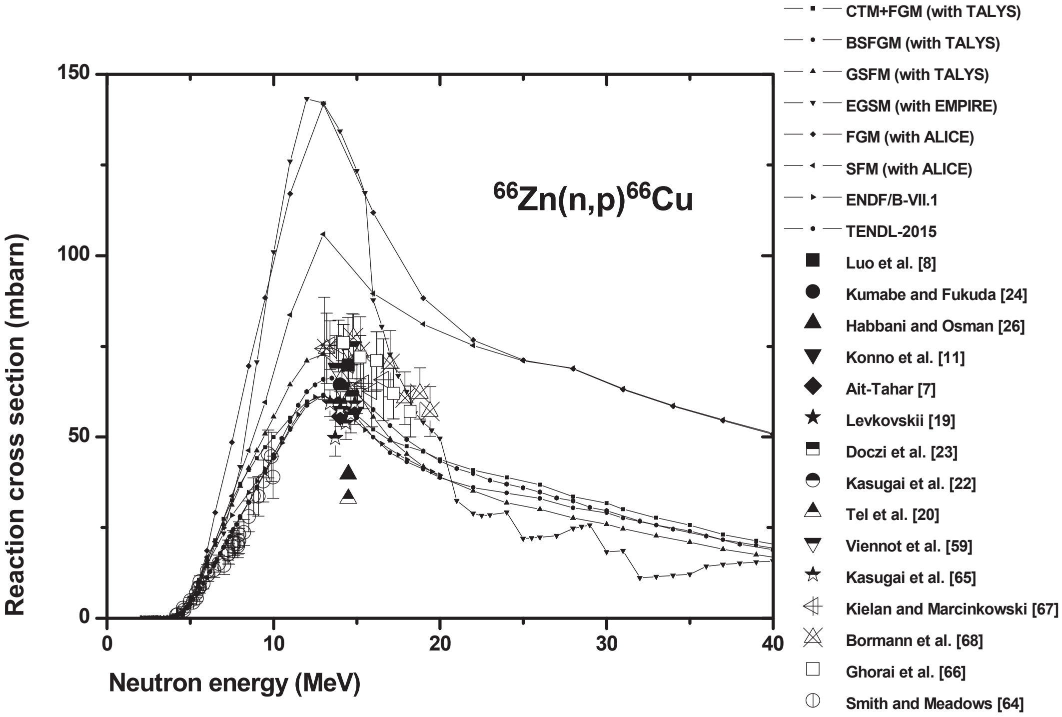

Fig. 5. Cross-section predictions and experimental data [78] for ^{66}Zn(n,p)^{66}Cu nuclear reaction.

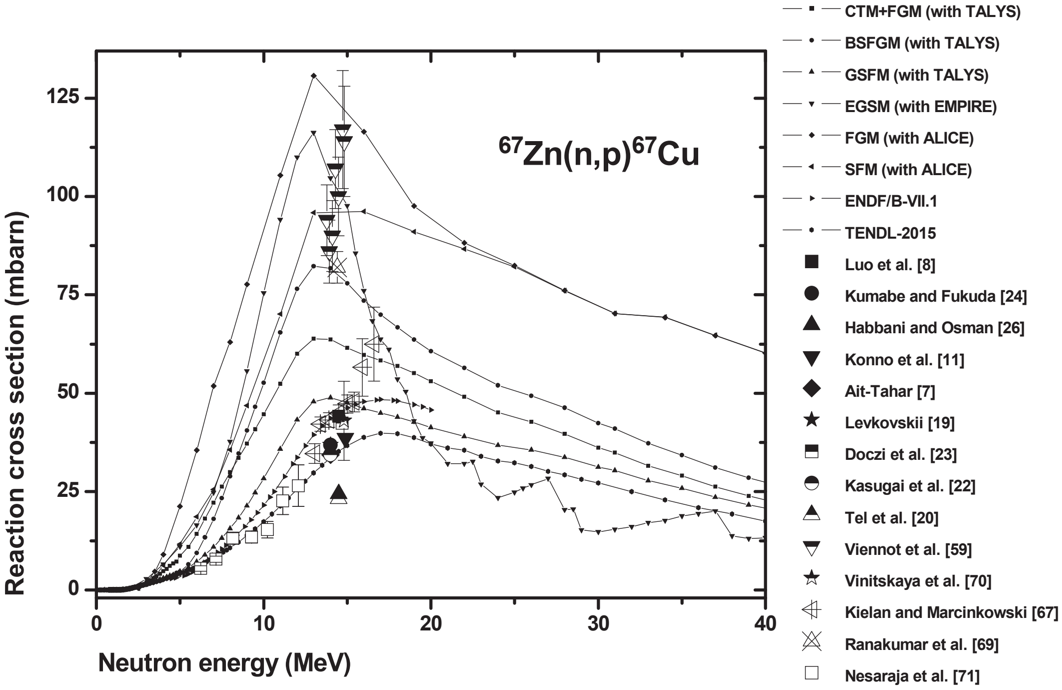

Fig. 6. Cross-section predictions and experimental data [78] for ^{67}Zn(n,p)^{67}Cu nuclear reaction.

Viennot et al. [59]. Moreover, the BSFGM nuclear-level density prediction of the exciton model is in excellent agreement with the cross-section value of 82 ± 4 mb at 14.4 MeV reported by Ranakumar et al. [69]. In addition, the cross-section value of 43 ± 10 mb at 14.8 MeV of Vinitskaya et al. [70] seems compatible with the GSFM prediction, the TENDL and ENDF/B-VII.1 evaluations, and the systematic results except for those of Tel et al. [20] and Habbani and Osman [26]. The excitation function of Nesaraja et al. [71] shows an excellent harmony with the TENDL and ENDF/B-VII.1 evaluations. The experimental data of Kielan and Marcinkowski [67] at 13.04–15.9 MeV agree very well with the ENDF/B-VII.1 evaluation. In addition, the cross-section data of Kielan and Marcinkowski [67] at 16.6 MeV show good agreement with the CTM + FGM, BSFGM, and EGSM predictions.

3.7. ^{68}Zn(n,p)^{68}Cu nuclear reaction

Theoretical and experimental comparisons to predict the ^{68}Zn(n,p)^{68}Cu reaction cross section are given in Fig. 7 and Table 2. The cross-section value of 46 ± 5 mb reported by Casanova and Sanchez [72] at 14.1-MeV neutron energy is in good agreement with the excitation function prediction of the SFM and BSFGM level densities. The experimental data of Filatenkov et al. [73] have lower cross sections than those of the other experimental and theoretical excitation functions for the considered nuclear reaction. Furthermore, the calculated nuclear excitation functions show an increasing trend with the increase of energy up to an incident energy of 15 MeV. At this maximum cross-section region, the excitation functions obtained by EMPIRE and ALICE codes yield higher cross-section values. Three different cross-section predictions including BSFGM, GSFM, and CTM + FGM level densities, obtained using the TALYS code, and the TENDL and ENDF/B-VII.1 evaluations, are in very good harmony with the experimental data of Kielan and

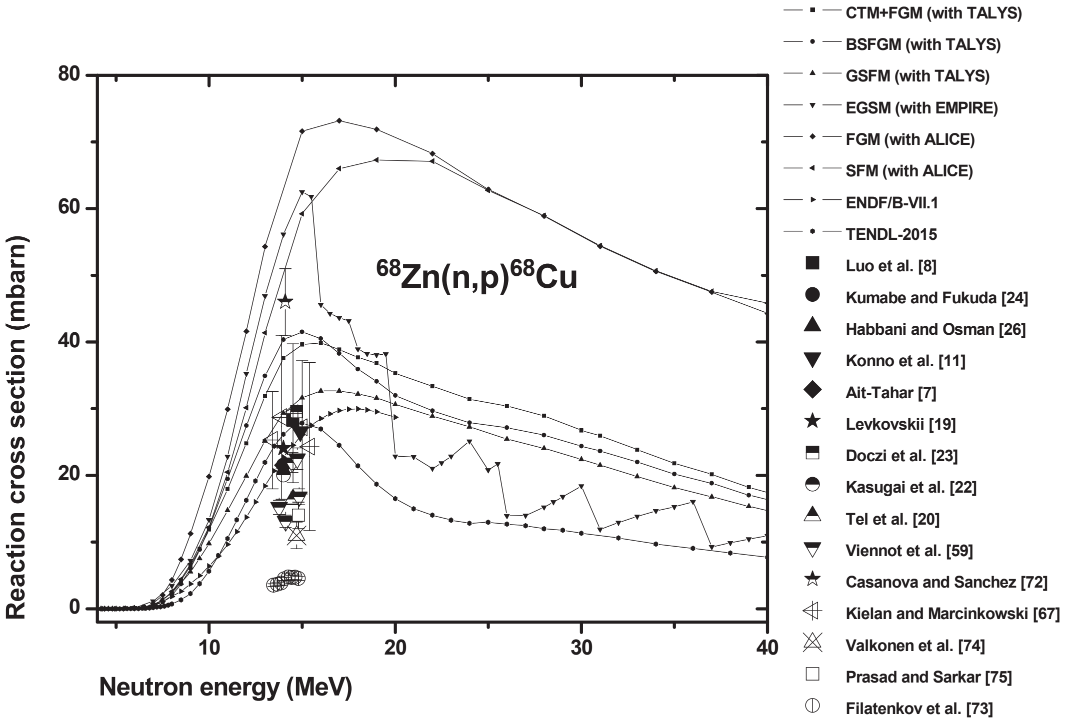

Fig. 7. Cross-section predictions and experimental data [78] for ^{68}Zn(n,p)^{68}Cu nuclear reaction.

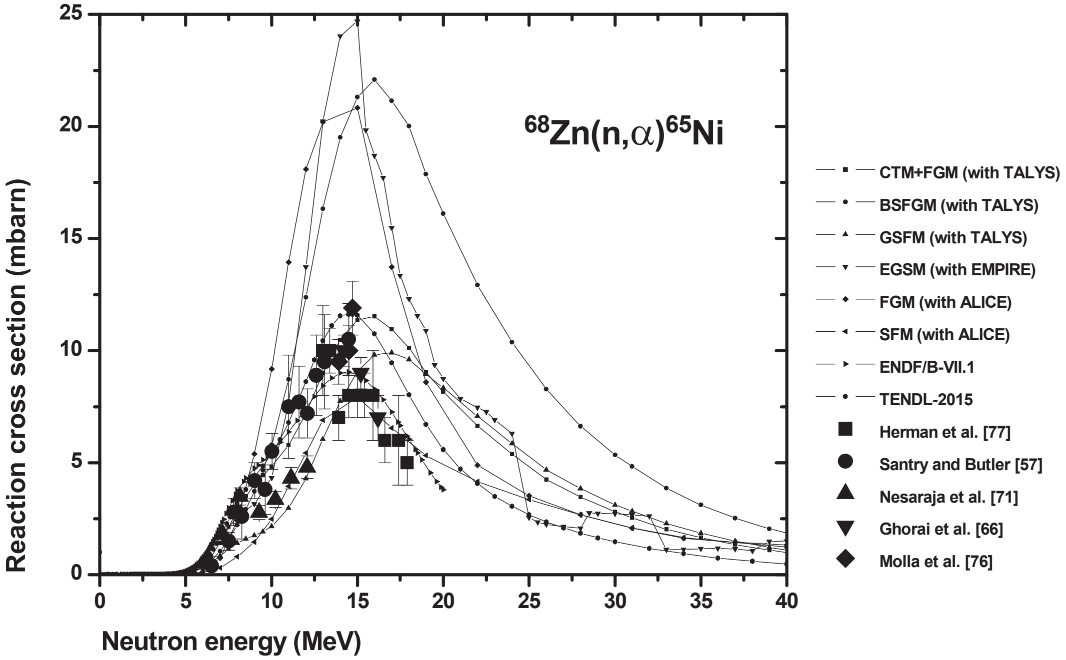

Fig. 8. Cross-section predictions and experimental data [78] for ^{68}Zn(n,α)^{65}Ni nuclear reaction.

Marcinkowski [67] within the experimental uncertainty. The measured data of Valkonen et al. [74] and Prasad and Sarkar [75] show very good agreement with the cross-section values obtained using the systematics of Tel et al. [20] and Habbani and Osman [26].

3.8. $^{68}Zn(n,\alpha)^{65}Ni$ nuclear reaction

All excitation functions for the ^{68}Zn(n,α)^{65}Ni nuclear reaction are plotted in Fig. 8. The nuclear excitation curves are somewhat affected by the use of different level densities in the model-based calculations. It can be seen that the FGM, EGSM, and BSFGM level density predictions with the GDH and exciton model are too high compared with the other cross-section data in the maximum region of the excitation curves of 12–18 MeV. The cross-section data obtained by CTM + FGM level density with the exciton model, and the evaluated data of TENDL and ENDF/B-VII.1 show results somewhat similar to measured data of Santry and Butler [57] and Molla et al. [76] for the considered nuclear reaction. The evaluated data of ENDF/B-VII.1 are consistent with the experimental results of Ghorai et al. [66] within the experimental uncertainties for the incident energies of 14.2–16.2 MeV. By contrast, the ENDF/B-VII.1 library and SFM calculations show a close agreement with the measured cross-section data reported by Herman et al. [77]. In addition, the CTM + FGM level density predictions and the TENDL library are consistent with the experimental results of Nesaraja et al. [71] at energies of 6.24 MeV, 7.16 MeV, and 8.16 MeV. By contrast, the experimental values of Nesaraja et al. [71] at energies of 10.23 MeV, 11.15 MeV, and 12.08 MeV are in a good harmony with the SFM level density calculations performed using the GDH model via ALICE code.

4. Conclusion

The cross sections of some nuclear reactions induced by neutrons on zinc were calculated using important pre-equilibrium nuclear models. A careful and systematic set of model calculations was obtained for the nuclear reaction cross sections. It can be said that the pre-equilibrium approaches are dominant in the investigated excitation energy region. In addition, the excitation functions obtained by pre-equilibrium models in the calculations are highly affected by the use of different level densities when the probability of nuclear reaction is high. Therefore, the level densities have a strong effect on the reaction cross section. By contrast, it seems that the selection of an accurate cross section systematic for the (n,2n) and (n,p) neutron reactions is very important for obtaining the correct excitation functions. In addition, exciton model predictions are generally successful for these nuclear reactions. We believe that these new sets of calculated cross-section data can help in understanding these neutron reactions.

Conflicts of interest

The authors have no conflicts of interest to declare.

References

[1] M. Yiğit, E. Tel, İ.H. Sarpün, Excitation function calculations for α+^{93}Nb nuclear reactions, Nucl. Instrum. Methods Phys. Res. B 385 (2016) 59–64.

[2] M. Yiğit, E. Tel, Reaction cross sections in the interactions of neutrons with Yttrium nucleus, J. Radioanal. Nucl. Chem. 306 (2015) 203–211.

[3] M. Yiğit, Theoretical predictions of excitation functions of neutron-induced reactions on 6Li, 9Be, 12C and 23Na nuclei at low energies, J. Fusion Energy 34 (2015) 140–147.

[4] M. Yiğit, E. Tel, Nuclear model calculation for production of ^{18}F, ^{22}Na, ^{44,46}Sc, ^{54}Mn, ^{64}Cu, ^{68}Ga, ^{76}Br and ^{90}Y radionuclides used in medical applications, Ann. Nucl. Energy 69 (2014) 44–50.

[5] J. Luo, F. Tuo, X. Kong, Activation cross sections and isomeric cross section ratios for ^{184}Os(n,2n)^{183m,g}Os, ^{190}Os(n,p)^{190m,g}Re and ^{86}Sr(n,2n)^{85m,g}Sr reactions from 13.5 to 14.8 MeV, J. Radioanal. Nucl. Chem. 279 (2009) 443–454.

[6] Y. Song, F. Zhou, M. Tian, Y. Li, S. Yuan, C. Lan, Measurements of the cross section for the ^{182}W(n,p)$^{182(m+g)}$Ta and ^{184}(n,p)^{184}Ta reactions in the 14 MeV energy range using the activation technique, Appl. Radiat. Isot 98 (2015) 29.

[7] S. Ait-Tahar, The systematics of (n,p) cross sections for 14 MeV neutrons, J. Phys. G Nucl. Part Phys. 13 (1987) 121–125.

[8] J. Luo, F. Tuo, F. Zhou, X. Kong, Semi-empirical systematics for the cross-sections of the reactions (n,α), (n,p) and (n,2n) at 14.5 MeV neutrons on the basis of experimental data measured by Lanzhou University, Nucl. Instrum. Methods Phys. Res. B 266 (2008) 4862–4868.

[9] E. Tel, Ş. Okuducu, M.H. Bölükdemir, G. Tanır, Semi-empirical systematics of (n, 2n),(n, α) reactions cross sections at 14–15 MeV neutron energy, Int. J. Mod. Phys. E 17 (2008) 567–583.

[10] A. Adam, L. Jeki, On the shell effect in (n,2n) reaction cross-sections, Acta Phys. Acad. Sci. Hung. 26 (1969) 335–338.

[11] C. Konno, Y. Ikeda, K. Osihi, K. Kawade, H. Yamamoto, H. Maekawa, Activation Cross Section Measurements at Neutron Energy From 13.3 to 14.9 Mev Using the FNS Facility, JAERI Rep. No. 1329, Japan Atomic Energy Research Institute, Tokyo, Japan, 1993.

[12] A. Kara, T. Korkut, M. Yiğit, E. Tel, Modelling study on production cross sections of ^{111}In radioisotopes used in nuclear medicine, Kerntechnik 80 (2015) 270–274.

[13] M. Eslami, T. Kakavand, M. Mirzaiic, Theoretical approach to study the light particles induced production routes of ^{22}Na, Ann. Nucl. Energy 83 (2015) 14–24.

[14] B. Demir, A. Kaplan, V. Çapalı, H. Özdoğan, İ.H. Sarpün, A. Aydın, E. Tel, Neutron production cross-section and Geant4 calculations of the structural fusion material ^{59}Co for (α, xn) and (γ, xn) reactions, J. Fusion Energy 34 (2015) 636–641.

[15] A. Kaplan, İ.H. Sarpün, A. Aydın, E. Tel, V. Çapalı, H. Özdoğan, (γ,2n)-Reaction cross-section calculations of several even-even lanthanide nuclei using different level density models, Phys. At. Nucl. 78 (2015) 53–64.

[16] C.H.M. Broeders, A. Yu Konobeyev, YuA. Korovin, V.P. Lunev, M. Blann, ALICE-ASH Manual (FZK 7183) [Internet], May 2006 [cited 2016 May 2]. Available from: http://bibliothek.fzk.de/zb/berichte/FZKA7183.pdf.

[17] A. Koning, S. Hilaire, S. Goriely, TALYS 1.6 Code [Internet], 2013 [cited 2016 May 2]. Available from: http://www.talys.eu/download-talys/.

[18] M. Herman, R. Capote, M. Sin, A. Trkov, B. Carlson, D. Brown, G. Nobre, P. Oblozinsky, C. Mattoon, H. Wienke, S. Hoblit, Y.-S. Cho, V. Plujko, V. Zerkin, EMPIRE-3.2 (Malta) [Internet], 2013 [cited 2016 May 2]. Available from: http://www.nndc.bnl.gov/empire/main.html.

[19] V.N. Levkovskii, Empirical Behavior of the (n, p) Cross Section for 14-15 MeV Neutrons, JETP Sov. Phys. 18 (1964) 213–217.

[20] E. Tel, B. Şarer, Ş. Okuducu, A. Aydın, G. Tanır, A new empirical formula for 14–15 MeV neutron-induced (n,p) reaction cross sections, J. Phys. G Nucl. Part Phys. 29 (2003) 2169–2177.

[21] W. Lu, R.W. Fink, Applicability of the constant-nuclear-temperature approximation in statistical-model calculations of neutron cross sections at 14.4 MeV for medium-z nuclei, Phys. Rev. C 4 (1971) 1173.

[22] Y. Kasugai, Y. Ikeda, H. Yamamoto, K. Kawade, Systematics for (n,p) excitation functions in the neutron energy between 13.3 and 15.0 MeV, Ann. Nucl. Energy 23 (1996) 1429–1444.

[23] R. Doczi, V. Semkova, A.D. Majdeddin, C.M. Buczko, J. Csikai, Investigations on (n,p) Cross Sections in the 14 MeV Region, INDC(HUN)-032, IAEA-NDS, 1997. Vienna, Austria.

[24] I. Kumabe, K.J. Fukuda, Empirical formulas for 14-MeV (n,p) and (n,α) cross sections, Nucl. Sci. Tech. 24 (1987) 839–843.

[25] V.M. Bychkov, V.N. Manokhin, A.B. Pashchenko, V.I. Plyashin, Cross Sections for the (n,p), (n,a) and (n,2n) Threshold Reactions, INDC(CCP)-146, IAEA-NDS, 1980. Vienna, Austria.

[26] F.I. Habbani, K.T. Osman, Systematics for the cross-sections of the reactions (n,p),(n, α) and (n, 2n) at 14.5 MeV neutrons, Appl. Radiat. Isot. 54 (2001) 283–290.

[27] M.K. Sharma, H.D. Bhardwaj, Unnati, P.P. Singh, B.P. Singh, R. Prasad, A study of preequilibrium emission of neutrons in ^{93}Nb(α, xn) reactions, Eur. Phys. J. A 31 (2007) 43–51.

[28] J.J. Griffin, Statistical model of intermediate structure, Phys. Rev. Lett. 17 (1966) 478.

[29] A.J. Koning, M.C. Duijvestijn, A global pre-equilibrium analysis from 7 to 200 MeV based on the optical model potential, Nucl. Phys. A 744 (2004) 15.

[30] M. Blann, H.K. Vonach, Global test of modified pre-compound decay models, Phys. Rev. C 28 (1983) 1475–1492.

[31] A.V. Ignatyuk, K.K. Istekov, G.N. Smirenkin, The role of collective effects for nuclear level density systematics, Yadernaja Fizika 29 (1979) 875.

[32] A. D'Arrigo, G. Giardina, M. Herman, A.V. Ignatyuk, A. Taccone, Semi-empirical determination of the shell correction temperature and spin dependence by means of nuclear fission, J. Phys. G 20 (1994) 365.

[33] A. Gilbert, A.G.W. Cameron, A composite nuclear-level density formula with shell corrections, Can. J. Phys. 43 (1965) 1446.

[34] W. Dilg, W. Schantl, H. Vonach, M. Uhl, Level density parameters for the back-shifted fermi gas model in the mass range 40, Nucl. Phys. A 217 (1973) 269.

[35] A.V. Ignatyuk, J.L. Weil, S. Raman, S. Kahane, Density of discrete levels in ^{116}Sn, Phys. Rev. C 47 (1993) 1504.

[36] A.V. Ignatyuk, K.K. Istekov, G.N. Smirenkin, The role of collective effects in the systematics of nuclear level densities, Sov. J. Nucl. Phys. 29 (1979) 450.

[37] C.K. Cline, M. Blann, The pre-equilibrium statistical model: description of the nuclear equilibration process and parameterization of the model, Nucl. Phys. A 172 (1971) 225.

[38] C.K. Cline, Extensions to the pre-equilibrium statistical model and a study of complex particle emission, Nucl. Phys. A 193 (1972) 417.

[39] I. Ribansky, P. Oblozhinsky, E. Betak, Pre-equilibrium decay and the exciton model, Nucl. Phys. A 205 (1973) 545.

[40] M. Yiğit, E. Tel, A systematic study for cross sections on (d,2n) nuclear reactions between 11.57 and 18.91 MeV, J. Fusion Energy 35 (2016) 585–590.

[41] M. Yiğit, Empirical formula on (n,^{3}He) reaction cross sections at 14.6 MeV neutrons, Appl. Radiat. Isot. 105 (2015) 15–19.

[42] M. Yiğit, E. Tel, Cross section systematics of (d,p) reactions at 8.5 MeV, Nucl. Eng. Des. 280 (2014) 37–41.

[43] M. Yiğit, E. Tel, A study on empirical systematic for the (d,n) reaction cross sections at 8.6 MeV, Kerntechnik 79 (2014) 488–493.

[44] C.H.M. Broeders, A.Yu Konobeyev, Systematics of (p,α) (p,nα), and (p,np) reaction cross sections, Appl. Radiat. Isotop. 6 (2007) 1249.

[45] ENDF (Evaluated Nuclear Data File) [Internet], ENDF/B–VII.1 (USA), 2011 [cited 2017 May 2]. Available from: http://www.nndc.bnl.gov/exfor/endf00.jsp.

[46] A.J. Koning, D. Rochman, J. Kopecky, J. Ch Sublet, M. Fleming, E. Bauge, S. Hilaire, P. Romain, B. Morillon, H. Duarte, S.C. vanderMarck, S. Pomp, H. Sjostrand, R. Forrest, H. Henriksson, O. Cabellos, S. Goriely, J. Leppanen, H. Leeb, A. Plompen, R. Mills, TALYS-Based Evaluated Nuclear Data Library (TENDL) Data Library [Internet], 2015 [cited 4 May 2017]. Available from: https://tendl.web.psi.ch/tendl_2015/tendl2015.html.

[47] Y. Uwamino, H. Sugita, Y. Kondo, T. Nakamura, Measurement of neutron activation cross sections of energy up to 40 MeV using semimonoenergetic p-Be neutrons, Nucl. Sci. Eng. 111 (1992) 391.

[48] A.V. Cohen, P.H. White, The excitation curves of some (n,p) processes induced by neutrons of 12.5-17.5 Mev energy, Nucl. Phys. 1 (1956) 73.

[49] A. Paulsen, H. Liskien, Excitation functions for the reactions ^{58}Ni(n,2n)^{57}Ni, ^{65}Cu(n,2n)^{64}Cu and ^{64}Zn(n,2n)^{63}Zn in the Energy Range 12.6 to 19.6 MeV, Nukleonik 7 (1965) 117.

[50] C. Bhatia, W. Tornow, Measurement of the ^{64}Zn(n,2n)^{63}Zn reaction cross section between 12.5 and 14.5 MeV, J. Phys. G 40 (2013) 065104.

[51] W. Mannhart, D. Schmidt, Measurement of Neutron Activation Cross Sections in the Energy Range from 8 MeV to 15 MeV, Neutronenphysik Rep. No. 53, Physikalisch-Technische Bundesanstalt (PTB), Braunschweig, Germany, 2007.

[52] M. Bormann, B. Lammers, Excitation functions of (n,p) and (n,2n) reactions for some isotopes of K, Mn, Zn and Cu, Nucl. Phys. A 130 (1969) 195.

[53] T. Shiokawa, M. Yagi, H. Kaji, T. Sasaki, The ^{19}F(n,2n)^{18}F reaction as a 14-MeV neutron flux monitor, J. Inorg. Nucl. Chem. 30 (1968) 1.

[54] J. Vrzalova, O. Svoboda, A. Krasa, A. Kugler, M. Majerle, M. Suchopar, V. Wagner, Studies of (n,xn) cross-sections in Al, Au, Bi, Cu, Fe, I, In, Mg, Ni, Ta, Y, and Zn by the activation method, Nucl. Instrum. Methods Phys. Res. A 726 (2013) 84.

[55] T.S. Soewarsono, Y. Uwamino, T. Nakamura, Neutron Activation Cross Section Measurement from ^{7}Li(p,n) in the Proton Energy Region of 20 MeV to 40 MeV, JAERI Rep. No. M-027, Japan Atomic Energy Research Institute, Tokyo, Japan, 1992, p. 354.

[56] X. Huang, W. Yu, X. Han, W. Zhao, H. Lu, J. Chen, Z. Shi, G. Tang, G. Zhang, The effect of low-energy neutrons on activation cross-section measurement,, Nucl. Sci. Eng. 131 (1999) 267–274.

[57] D.C. Santry, J.P. Butler, Excitation curves for the reactions of fast neutrons with zinc, Can. J. Phys. 50 (1972) 2536.

[58] F. Gabbard, B.D. Kern, Cross sections for charged particle reactions induced in medium weight nuclei by neutrons in the energy range 12-18 MeV, Phys. Rev. 128 (1962) 1276.

[59] M. Viennot, A.A. Haddou, A. Chiadli, G. Paic, Excitation functions of (N,P) reactions in the region 13.75 to 15 MeV for Ti, Fe and Ni isotopes, in: K.H. Bockhoff (Ed.), Proceedings of the International Conference on Nuclear Data for Science and Technology, Springer, Berlin, Germany, 1982, pp. 406–408.

[60] A. Paulsen, H. Liskien, R. Widera, Cross sections of (n,2n) reactions for Ti-46,Zn-66, In-115 and Au-197, Atomkernenergie 26 (1975) 34.

[61] L. Hanlin, Z. Wenrong, Y. Weixiang, Activation cross section of Zn and Zr for 13-18 MeV neutrons, Chin. J. Nucl. Phys. 13 (1991) 11.

[62] M. Wagner, G. Winkler, H. Vonach, Cs M. Buczko, J. Csikai, Measurement of the cross sections for the reactions ^{52}Cr(n,2n)^{51}Cr, ^{66}Zn(n,2n)^{65}Zn, ^{89}Y(n,2n)^{88}Y and ^{96}Zr (n,2n)^{95}Zr from 13.5 to 14.8 MeV, Ann. Nucl. Energy 16 (1989) 623.

[63] J. Csikai, G. Peto, Influence of direct inelastic scattering on (n,2n) cross sections, Acta Phys. Hung. 23 (1967) 87.

[64] D.L. Smith, J.W. Meadows, Activation cross sections for ^{66}Zn(n,p) ^{66}Cu, Nucl. Sci. Eng. 76 (1980) 61.

[65] Y. Kasugai, H. Yamamoto, K. Kawade, T. Iida, Measurements of (n,p) cross-sections for short-lived products by 13.4–14.9 MeV neutrons, Ann. Nucl. Energy 25 (1998) 23.

[66] S.K. Ghorai, P.M. Sylva, J.R. Williams, W.L. Alford, Partial neutron cross sections for 64Zn, 66Zn, 67Zn and 68Zn between 14.2 and 18.2 MeV, Ann. Nucl. Energy 22 (1995) 11.

[67] D. Kielan, A. Marcinkowski, Cross sections for the (n,p) reaction on zinc isotopes in terms of the novel multistep compound reaction model, Z. Phys. A 352 (1995) 137.

[68] M. Bormann, E. Fretwurst, P. Schehka, G. Wrege, H. Büttner, A. Lindner, H. Meldner, Some excitation functions of neutron induced reactions in the energy range 12.6–19.6 MeV, Nucl. Phys. 63 (1965) 438–448.

[69] N. Ranakumar, E. Kondaiah, R.W. Fink, 14 MeV cross sections of silicon and zinc isotopes, Bull. Am. Phys. Soc. 13 (1968) 602.

[70] G.P. Vinitskaya, V.N. Levkovskiy, V.V. Sokolskiy, I.V. Kazachevskiy, Cross sections of the (n,p) and (n,a) reactions at neutron energy 14.8 MeV, Yadernaya Fizika 6 (1967) 240.

[71] C. Nesaraja, K.H. Linse, S. Spellerberg, S. Sudar, A. Suhaimi, J. Csikai, A.Fessler, S.M. Qaim, Excitation functions of neutron induced reactions on some isotopes of zinc, gallium and germanium in the energy range of 6.2 to 12.4 MeV, Radiochim. Acta 86 (1999) 1.

[72] J.L. Casanova, M.L. Sanchez, Measurement of the (n,p), (n,a), (n,2n) cross sections of Zn, Ga, Ge, As and Se for 14.1 MeV neutrons and (n,p) cross section analysis, An. Fisicay Quim 72 (1976) 186.

[73] A.A. Filatenkov, S.V. Chuvaev, V.N. Aksenov, V.A. Jakovlev, Systematic Measurement of Activation Cross Sections at Neutron Energies from 13.4 to 14.9 MeV. reportKhlopin Radiev Institute Leningrad Rep. No. 252, 1999.

[74] M. Valkonen, P. Homberg, R. Rieppo, J.K. Keinaenen, J. Kantele, Studies of 14 MeV Neutron Activation Cross Sections with Special Reference to the Capture Reaction, reportRep. No. 1, Department of Physics, University of Jyvaeskylae, 1976.

[75] R. Prasad, D.C. Sarkar, Measured (n,p) reaction cross-sections and their predicted values at 14. 8 MeV, Nuovo Cimento A 3 (1971) 467.

[76] N.I. Molla, R.U. Miah, S. Basunia, S.M. Hossain, M. Rahman, Cross Sections of (n,p), (n,a) and (n,2n) Processes on Scandium, Vanadium, Cobalt, Copper and Zinc Isotope in the Energy Range 13.57–14.71 MeV, International Conference on Nuclear Data for Science and Technology vol. 2, American Nuclear Society, La Grange Park, IL, 1994, p. 938.

[77] M. Herman, A. Marcinkowski, J. Dresler, U. Garuska, Cross sections for the fast neutron induced reactions on Si and Zn isotopes, Rep. No. 1871, Inst. Badan Jadr. (Nucl. Res.) (1980) 13. Swierk Warsaw.

[78] Experimental Nuclear Reaction Data (EXFOR) [Internet], 2016 [cited 2016 May 2]. Available from: http://www.nndc.bnl.gov/exfor/exfor.htm.